STARS

University of Central Florida
STARS

Retrospective Theses and Dissertations

1973

Detection of Gallium Arsenide Semiconductor Laser Pulses with Avalanche Detectors

Albert Henry Marshall
University of Central Florida

 Part of the Education Commons
Find similar works at: https://stars.library.ucf.edu/rtd
University of Central Florida Libraries http://library.ucf.edu

This Masters Thesis (Open Access) is brought to you for free and open access by STARS. It has been accepted for inclusion in Retrospective Theses and Dissertations by an authorized administrator of STARS. For more information, please contact STARS@ucf.edu.

STARS Citation
Marshall, Albert Henry, "Detection of Gallium Arsenide Semiconductor Laser Pulses with Avalanche Detectors" (1973). *Retrospective Theses and Dissertations*. 64.
https://stars.library.ucf.edu/rtd/64

DETECTION OF GALLIUM ARSENIDE SEMICONDUCTOR LASER PULSES WITH AVALANCHE DETECTORS

BY

ALBERT HENRY MARSHALL
B.A., Montclair State College, 1954
M.A.T., Brown University, 1962
M.S., Drexel Institute of Technology, 1965

THESIS

Submitted in partial fulfillment of the requirements
for the degree of Master of Science
in the Graduate Studies Program of
Florida Technological University

Orlando, Florida
1973

ACKNOWLEDGMENT

The author expresses sincere thanks to his advisor, Dr. Ronald Phillips, Florida Technological University, for his excellent advice, encouragement and helpful criticisms. I also wish to thank Mic Shore for her effort in typing the final manuscript.

130481

TABLE OF CONTENTS

LIST OF FIGURES

1. INTRODUCTION

With the increasing application of pulsed semiconductor lasers to voice communications, laser altimeters and weapon fire simulation, there has developed a requirement for a very high-speed sensitive detector of modulated light. In particular the detector must respond to nanosecond pulses in the near-infrared spectrum, have a high quantum efficiency and be limited by only the detectors shot noise. Previous techniques and devices for accomplishing these laser detection requirements include the photomultiplier, photoconductive detectors and reverse biased P-I-N photodiodes.

The photomultiplier tube until the recent development of avalanche photodiodes most nearly meets these requirements; however, since the gallium arsenide, semiconductor laser operates at 904 nm at room temperature or in the near infrared, the photomultipliers quantum efficiency is quite low. Detectors utilizing the photoconductive effect are not suitable because they are limited at present to frequencies below the microwave range and are narrow band devices. The P-I-N photodiode is suitable for detection of these pulses but they have no inherent gain and are thermal noise limited. Avalanche photodiodes can provide gain and are best suited for low-level detection of Gallium-Arsenide laser pulses.

The avalanche photodiode is especially suited for low-noise application where the principal noise source is the preamplifier. Avalanche photodiodes have characteristics similar to a conventional

photodiode with the addition of an internal linear current-gain mechanism due to the avalanche effect. The gain is determined by the applied reverse bias which is just below the breakdown voltage of the diode. Signal current gain in avalanche detectors greatly improves the sensitivity of the laser receiver.

This thesis will discuss the theory of avalanche detectors, performance, and the design of a laser receiver for the detection of reflected gallium-arsenide semiconductor laser pulses.

2. SILICON AVALANCHE DETECTOR THEORY AND STRUCTURE

Signal enhancement through avalanche multiplication in a P-I-N photodiode was reported for the first time by Kenneth Johnson in 1964[1]. He obtained carrier multiplication by operating a silicon photodiode at a voltage where some carrier multiplication occurred, and was able to improve the output signal-to-noise ratio. Since this time much has been accomplished to optimize the avalanche type detector. The avalanche breakdown effect is similar to the Townsend discharge in gas filled tubes and relies on the formation of carriers on impact collision of atoms by other carriers which have been imparted sufficient energy by an electric field. If a free electron and hole is created by an absorbed photon within the depletion layer of the diode junction, and an electric field is applied, the carriers will increase their velocity and kinetic energy because of the electric field. As the carriers move in the lattice structure inside the semiconductor, the free carrier may collide with an atom within the junction and, because of their high energy level they can rip off additional carriers from the atom. The free carriers essentially "kick" new electrons from the valence to the conduction band, while still transversing the depletion layer. Providing sufficient energy still remains in the original colliding carrier, additional collisions and thus other carriers will be freed from additional atoms. The newly released carriers now gain sufficient energy from the field to

begin collisions of their own. Thus, multiplication of the carriers has occurred and its degree is a function of how near to the breakdown voltage the diode is biased. [2]

The carrier multiplication can also be explained using an energy-position diagram (Figure 1). An absorbed photon (A) creates an electron-hole pair and the electron is accelerated by the high field strength until at a point (C) it has gained sufficient kinetic energy to excite an electron from the valence to the conduction band, thus creating a new electron-hole pair. The newly generated carriers drift in turn, in opposite directions. The hole (F) can also cause carrier multiplication. This phenomenon causes a dramatic increase in junction current.

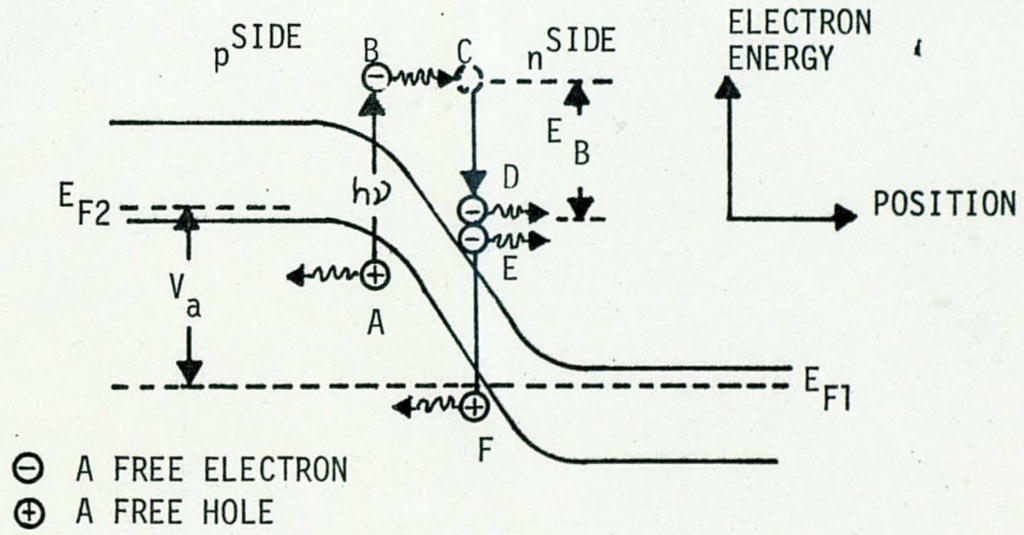

FIGURE 1. Energy-Position Diagram Illustrating Carrier Multiplication

Two types of breakdown can occur in diodes. In narrow p-n junctions an effect known as field emission was described by Zener in 1934. Zener's original theory was that under very intense electric fields (10^5 V/cm or greater), electrons are pulled out of the valence band and traverse the forbidden energy gap by quantum-mechanical tunneling. In avalanche diodes, with wider junctions, the newer theory of avalanche breakdown must be utilized.

In avalanche breakdown the junction does not suddenly begin to conduct very large currents all over the junction but rather at small discrete points. These small high-current-density discharges are called microplasmas. Microplasmas occur preferentially along areas of lattice damage at the junction [3].

An avalanche detector consists of a deep-diffused graded p-n junction in a silicon wafer. This type of diode is fabricated by diffusion of gallium into high resistivity n-type silicon. Quality of the silicon is of great importance because fluctuations in the doping (striations) can cause large variations in the electric field distribution and therefore, to large changes in avalanche gain over the sensitive area. Dislocations and other lattice defects cause premature avalanche breakdown in "microplasmas" and render the device useless at this point because of high noise current [4]. Recent advances in the growth of high resistivity, very uniformly doped silicon and careful processing techniques have resulted in high quantum efficiencies and very large

avalanche gains. Figure 2 shows a schematic representation of a silicon avalanche photodiode and the field profile of a typical avalanche detector.

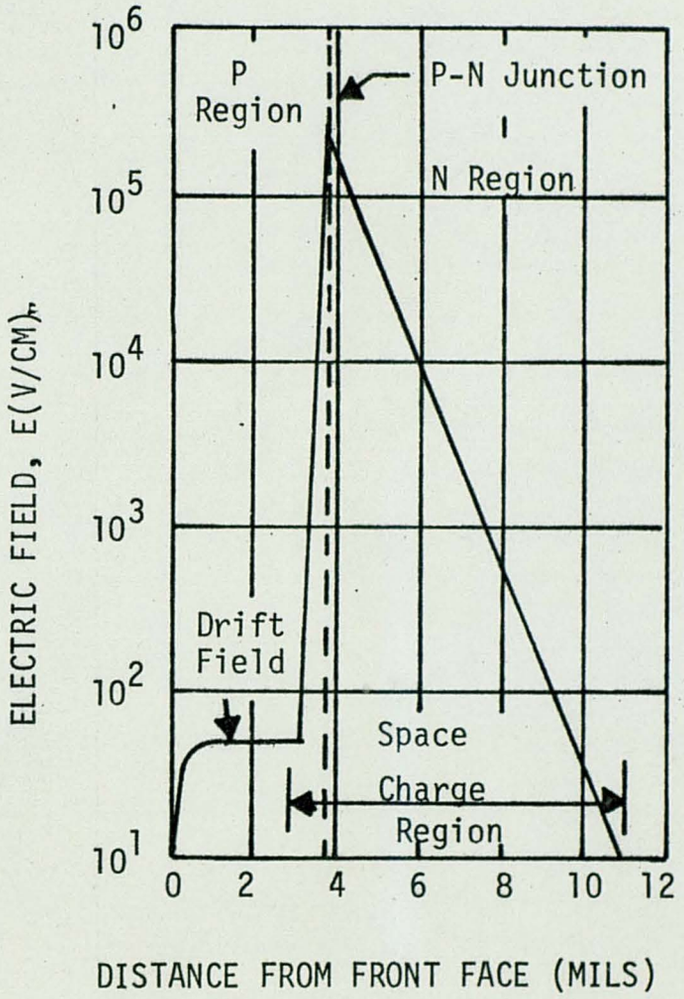

FIGURE 2. Schematic Representation of a Silicon Avalanche Photodiode and the Field Profile of a Typical Avalanche

The drift field in the p-region is caused by the concentration gradient of the gallium acceptor and is independent of the applied bias voltage. The drift field collects the charge carriers liberated by a photon in the depletion region and sweeps them into the space charge region where they are amplified in the high field. Electrical properties of the avalanche detector are determined by the field profile, space charge region, and the bulk leakage current through the detector.

A drift field of 50 volts/cm will cause an electron liberated by a photon to be swept toward the space charge region with a drift velocity (V drift).

V drift = μE (cm/sec)

V drift = 1350 cm^2/volt sec X 50 volts/cm

V drift = 6.75 X 10^4 cm/sec.

For this case a drift time of 37 nsec. per mil will occur.

The time delay of carriers crossing the high-field absorption region gives rise to a transit time cutoff frequency. The transit time across the depletion region of thickness $X_2 - X_1$ is given by

$$\tau = \frac{X_2 - X_1}{V_{drift}}$$

The drift time is a function of where the ionizing event occurs. When the carriers reach the p-n junction most of the gain process occurs in about 0.2 nanosecond, in this high field region. Following multiplication the electrons are located in the conduction

band and the n-region acts like an ordinary fifty ohm conductor, and no further time delays are present. The field profile in Figure 2 will not be the same at every point in the detector because variations in the crystal resistivity causes changes in the field profile, which leads to some variations in the avalanche gain across the face of the detector.

As reverse bias is applied to the detector, the space charge region begins to build up, and an effective capacitance appears across this region. The capacitance is analogous to a parallel plate capacitor whose plates correspond to the space charge region boundary, filled with a dielectric whose dielectric constant is that of silicon. As the detector bias is increased, the space charge region becomes thicker, and the capacitance decreases, since it is inversely proportional to the thickness.

Capacitance of the diode depletion region can be calculated from

$$C = \frac{\epsilon A}{X_2 - X_1}$$

where

ϵ = permitivity of semiconductor material,

A = area of avalanche diode,

$X_2 - X_1$ = thickness of active region.

Due to the dimensions of the avalanche photodiode the frequency response is limited by the transient-time effects and not by the RC cutoff.

The detector used has a capacitance of 8 pf. near avalanche. Figure 3 illustrates how the capacitance varies as a function of the applied reverse bias voltage. [5] Capacitance varies inversely as the square root of the voltage.

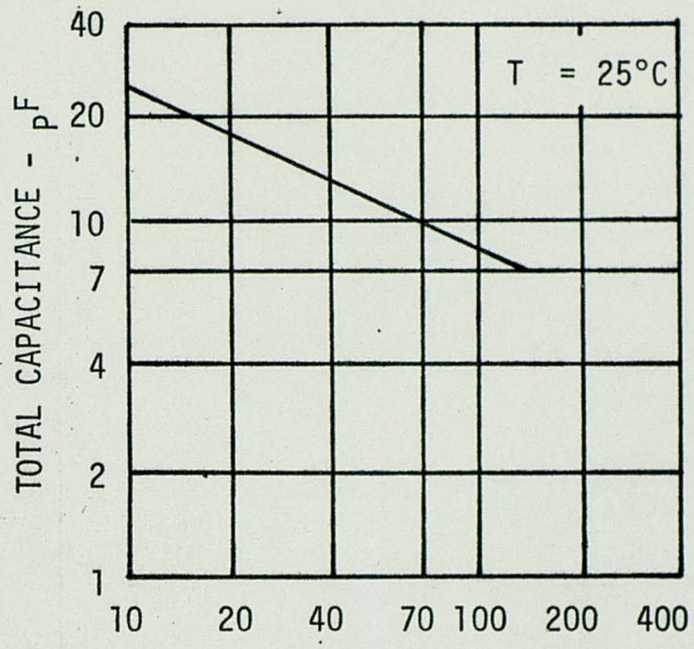

FIGURE 3. Effect of Reverse Bias on Detector Capacitance

When a photon enters the detector, the internal quantum efficiency is based on Lambert's Law. This law states that when light enters any thin layer of material perpendicular to the direction of propagation, the intensity is reduced proportional to the thickness of the layer. The photon flux after having penetrated the detector to a distance X is:

$$\Phi(x) = \Phi_o e^{-\alpha x}$$

where

Φ = photon flux incident on the detector,

α = absorption coefficient.

This formulation neglects both front-surface and internal reflections. Assuming each photon absorbed generates a hole-electron pair the quantum efficiency η, is

$$\eta = 1 - e^{-\alpha X_m}$$

The quantum efficiency of the avalanche detector is 70 percent at 0.9 microns.

The quantum efficiency varies as a function of the wavelength of the incident radiation. Silicon has an excellent quantum efficiency at the frequency of GaAs lasers (0.9 μm at 25°C). A plot of the normalized quantum efficiency versus wavelength is shown in Figure 4.

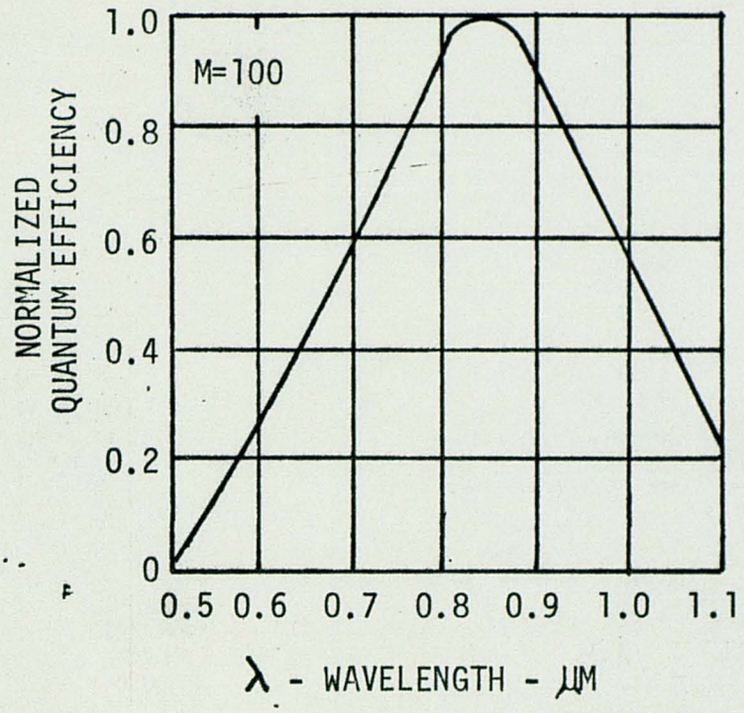

FIGURE 4. Normalized Quantum Efficiency vs. Wavelength

Functionally the avalanche detector can be thought of as a p-type region which acts to collect the charge, followed by a variable (0 to 80 nanosec.) delay line. The n-type region can be considered a pre-amplifier with a gain figure, proportional to avalanche multiplication, M. A functional representation of the detector is shown in Figure 5.

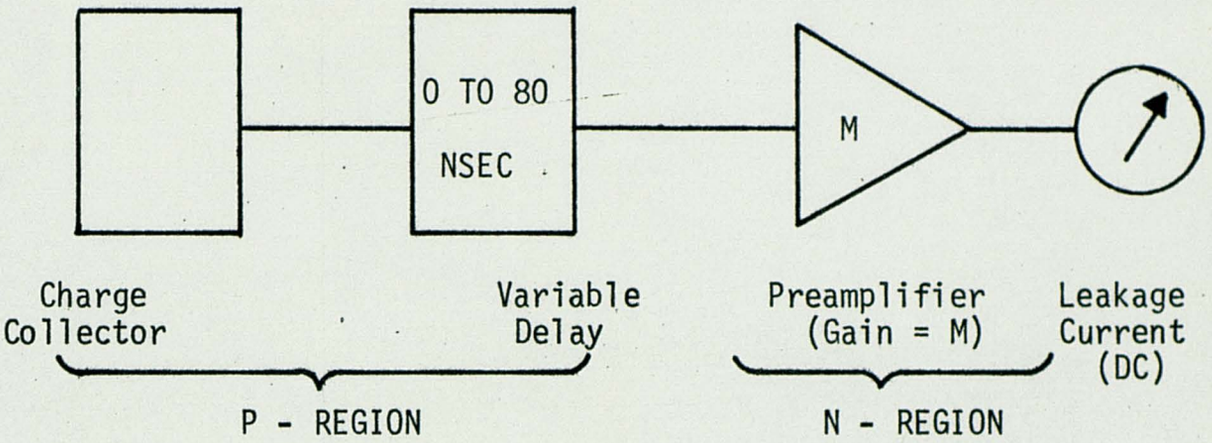

FIGURE 5. Functional Representation of an Avalanche Photodiode.

3. PERFORMANCE CHARACTERISTICS OF AVALANCHE DETECTORS

At bias voltages much below avalanche, the silicon avalanche detector exhibits characteristics similar to other large depletion layer silicon photodiodes. However, as the avalanche photodiode bias is increased, the responsivity, gain and dark current change as a function of the bias voltage.

Figure 6 shows a plot of signal power versus photocurrent gain. Figure 7 shows the photocurrent gain versus reverse detector bias [5].

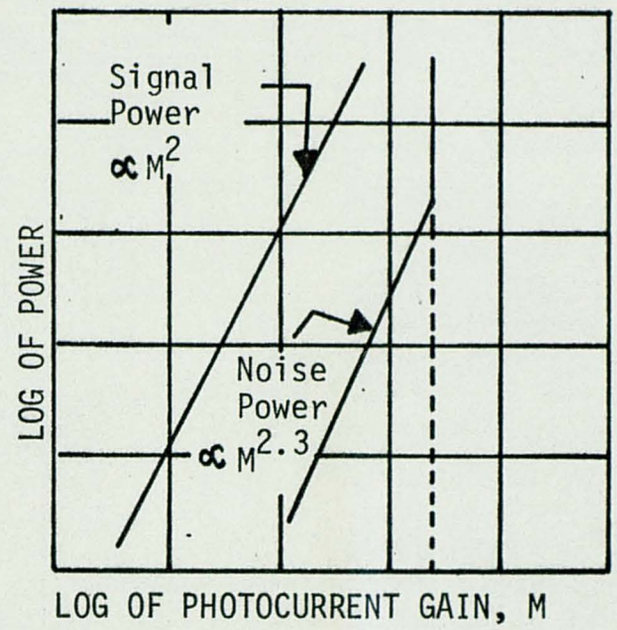

FIGURE 6. Signal Power and Noise Power versus Photocurrent Gain

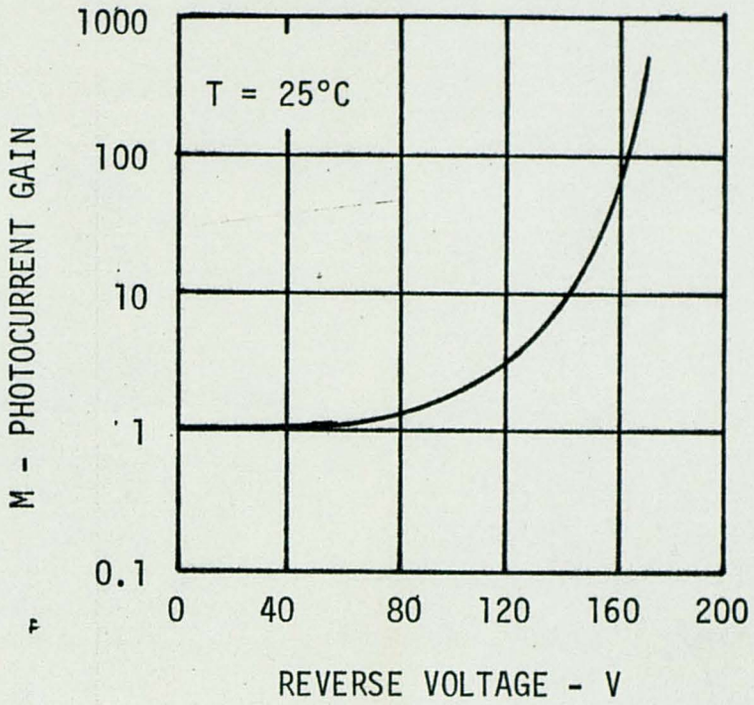

FIGURE 7. Photocurrent Gain versus Reverse Detector Bias

Multiplication by a factor M of the avalanche diodes photocurrent leads to an increase of M^2 of the signal power over the power which is normally available from a conventional photodiode. This effect is similar to that of the signal power from a photomultiplier, however, in this case, the avalanche gain M plays the role of the secondary electron multiplication gain. However, a problem arises because as shown in Figure 6, the noise does not increase as M^2, but as $M^{2.3}$. A theoretical study performed by McIntyre [6] predicted that if the multiplication is due to either holes or electrons then the multiplication factor of the signal power is M^2.

If both holes and electrons are equally effective in producing electron-hole pairs, then $M^{2.3}$ applies for this detector.

The ability to detect optical pulses with the avalanche detector is limited in accuracy by random fluctuations called noise. Three types of noise determine the minimum detectable signal in an optical receiver. The first is noise generated in the detector by the dark current. This noise increases dramatically at the breakdown voltage. The second type noise is induced by the recombination noise and is attributed to the random way in which electrons are generated in the detector.

In conventional photodiode receivers, the amplifier noise dominates, except for receivers having wide field of views, where the photon shot noise generated by the background can become larger than the amplifier noise. The dark noise of an avalanche detector is much smaller than the amplifier noise.

The avalanche photodiode is a high-impedance device, and for moderate values of avalanche gain, the equivalent parallel resistance of the diode is large compared to the normal circuit impedances. Therefore, the avalanche detector is a current source and the equivalent input noise current is the most useful parameter for describing the second-stage amplifier noise. The detector output goes to a low-noise high-speed transimpedance amplifier designed for current sources. The amplifier provides an output voltage which is linearly proportional to the detectors input current. A

schematic of the amplifier and diode detector is shown in Figure 8.

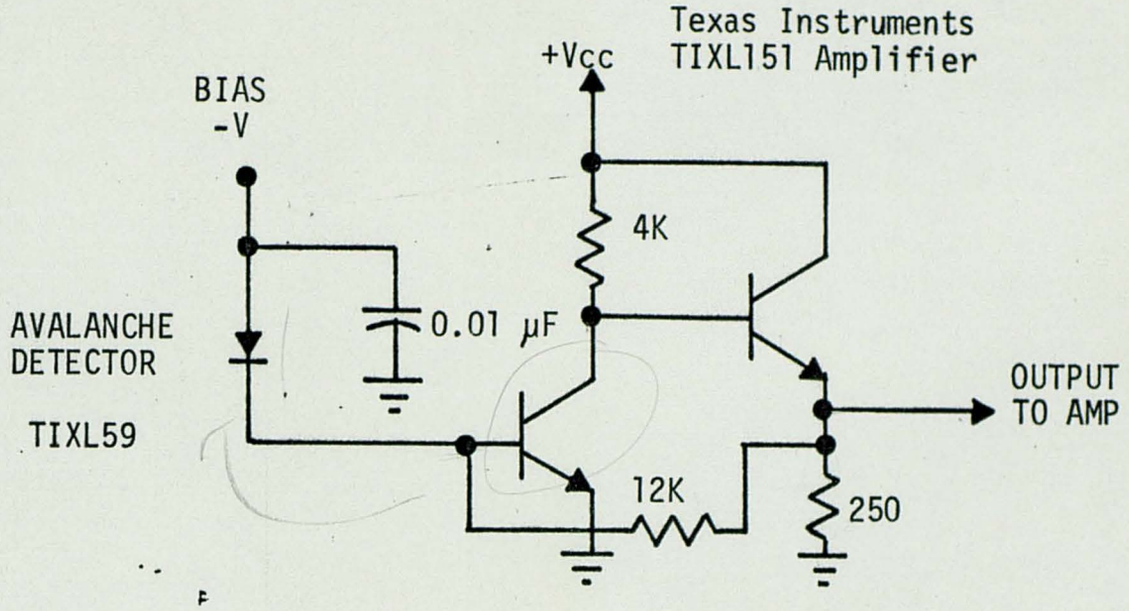

FIGURE 8. Schematic of Amplifier and Diode Detector

The input noise current of the amplifier is $i_x = 3 \times 10^{-12}$ A/√Hz. With a load resistance of 50 ohms the (-3dB) bandwidth is 18 MHz. The responsivity, R_0 are 0.5 Amperes/Watt at 0.9 μm (M=1). M is the multiplication factor which is 100 maximum. When the detector is <u>not</u> background limited one can determine the value of the noise equivalent power (NEP) of an avalanche receiver system. The amplifier noise can be expressed as a spectral noise current density, i_x, referred to the input of the amplifier, and its dimensions are A/√Hz. NEP is then defined as

$$NEP = \frac{i_x}{R_o M} = \frac{3 \times 10^{-12} \text{ A}/\sqrt{\text{Hz}}}{.5 \text{ A/W} \times 100} = 6 \times 10^{-14} \text{ W}/\sqrt{\text{Hz}}.$$

Therefore, in the absence of background, the combined diode and amplifier noise equivalent power is 6×10^{-14} $W/\sqrt{Hz}$.

The avalanche gain necessary for optimum signal to noise operation in the presence of background radiation incident on the detector will be determined next. Signal current, i_s, from the avalanche detector is given by, $i_s = P_{rcvd} R_o M$ where P_{rcvd} is the received laser signal power. The noise, i_n, is the sum of the dark noise and the noise current due to background radiation, P_{bgr} on the detector. The background noise is represented by $i_{bgr} = P_{bgr} R_o$. McIntyre's theory [6] states the system noise, i_n, is multiplied at a higher power then than the signal power, or $M^{2.3}$. Accordingly, the noise current can be expressed as

$$i_n = [2q(i_d + i_{bgr})M^{2.3}\Delta f]^{1/2}$$

where i_d is the dark current at M=1, q is the charge of an electron and Δf is the receiver bandwidth.

A schematic representation of the systems noise currents is shown in Figure 9.

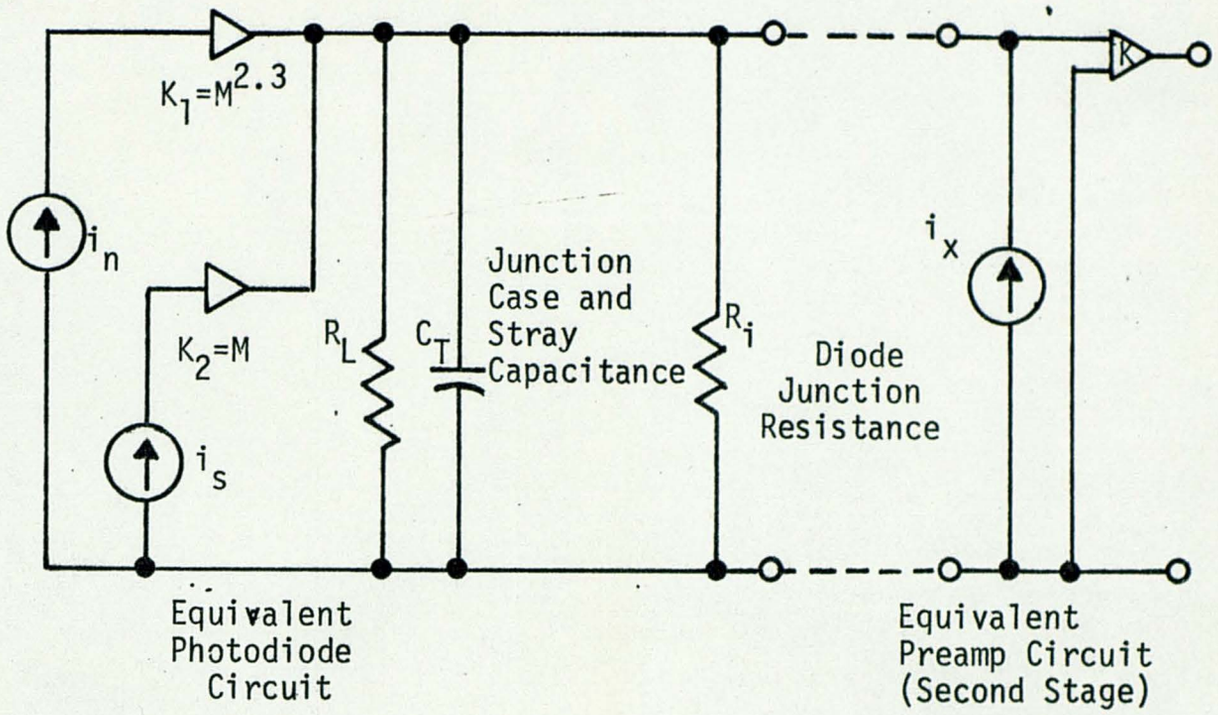

FIGURE 9. System Noise Currents

Signal-to-noise power ratio is given by

$$\left(\frac{i_s}{i_n}\right)^2 = \frac{(P_{rcvd} R_o M)^2}{[\,2q(i_d+i_{bgr})M^{2.3}\Delta f\,]}$$

The amplifier noise is given by $i_x^2 \Delta f$

Accounting for amplifier noise the signal-to-noise ratio for the receiver is

$$\left(\frac{i_s}{i_n}\right)^2 = \frac{P_{rcvd}^2 R_o^2 M^2}{[\,2q(i_d+P_{bgr}R_o)M^{2.3}+i_x^2\,]\Delta f}$$

Note that because $M^{2.3}$ occurs in the denominator, the denominator grows faster than the numerator and M is therefore limited as a

function of P_{bgr}, the optical background power incident on the detector. The optimum operating M is obtained when $\left(\frac{i_s}{i_n}\right)^2$ is a maximum. Multiplication gain at this condition is given by

$$M_{OPT} = \left[\frac{i_x^2}{(2.3-2)q\,(i_d + R_o P_{bgr})} \right]^{\frac{1}{2.3}}$$

Dark current is given by $i_d = 25 \times 10^{-12}$ amp.

Figure 10 is a plot of optimum gain versus background radiation.

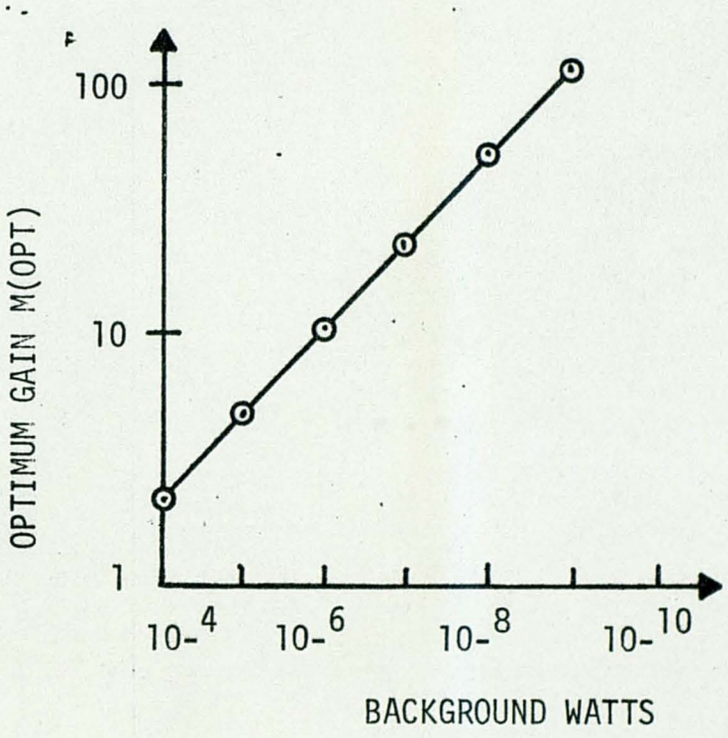

FIGURE 10. Optimum Gain, M(opt), versus Background Radiation

Effects of optical background radiation are minimized by utilizing a narrow band optical interference filter in front of the detector

optics and also a narrow field of view optical system for the receiver optics. These devices reduce the background noise and permit a greater detector gain, M.

The power received from a reflected laser beam, Prec can be expressed using the following equation, [7] for laser range finders

$$P_{rec} = \frac{P_t T_t \rho \cos\theta A_r T_r}{\pi R^2} \exp(-2\sigma R)$$

In this equation the two-way path transmittance loss through the atmosphere is given by exp(-2σR), and

P_t = peak transmitted laser power (watts)

T_t = transmittance of laser optics

R = range (m)

$\rho\cos\theta$ = target reflectance as a function of the angle of beam incidence to the target surface.

A_r = collecting area of receiver optics (m^2)

T_r = transmittance of receiver optics

Note that the power received can be increased by increasing the diameter of the collecting optical area. The receiver lens must also limit the field of view so a maximum M is realized. However, the field of view of the receiver optics should not be smaller than the laser beam on the target.

The background power is given by

$$P_{bgr} = \frac{H_{\lambda s} B_o \alpha_R^2 A_R T_R}{4} \rho \exp(-\sigma R)$$

where

$H_{\lambda s}$ = solar spectral irradiance (Wm^{-2} $\mathring{A}^{-1}$) at a given wavelength

B_o = pass band at the optical receiver

α_r = receiver beamwidth (rad)

Ar = collection area of receiver optics

Tr = transmittance of receiver optics

ρ = target reflectance

This equation assumes complete blocking except for the optical filter passband and ignores atmospheric backscattering. The background, Pgr can be seen to decrease as B_o, the filter bandwidth, is made narrower. A 15 nm filter with 70 percent transmissions is utilized in the system. A narrower interference filter could have been used in the receiver, but since the laser drifts .23 nm/°C, the 15nm filter was employed. A thermoelectric cooler can be utilized to temperature stabilize the laser. This permits operation with a narrower bandwidth interference filter.

4. GALLIUM ARSENIDE LASER TRANSMITTER.

This section of the thesis will describe the gallium arsenide laser transmitter. The transmitter produces laser pulses which are reflected and then detected by the avalanche detector system.

A gallium arsenide laser is a p-n diode in which a fraction of the injected minority carriers recombine by means of radiative transitions. The semiconductor laser is basically a planer p-n junction in a single crystal of gallium arsenide. Two of the parallel semireflective faces form a Fabry-Perot resonant cavity that enhances the optical Q of the system. The radiant flux is emitted from the thin rectangular area of the junction. The junction dimensions are determined by the semiconductor chip size; the longer dimension varies as a function of the chip size and the smaller dimension is determined by the carrier-diffusion distance, which is 2 μm in GaAs by doping level and junction configuration. The structure of a GaAs laser is shown in Figure 11.

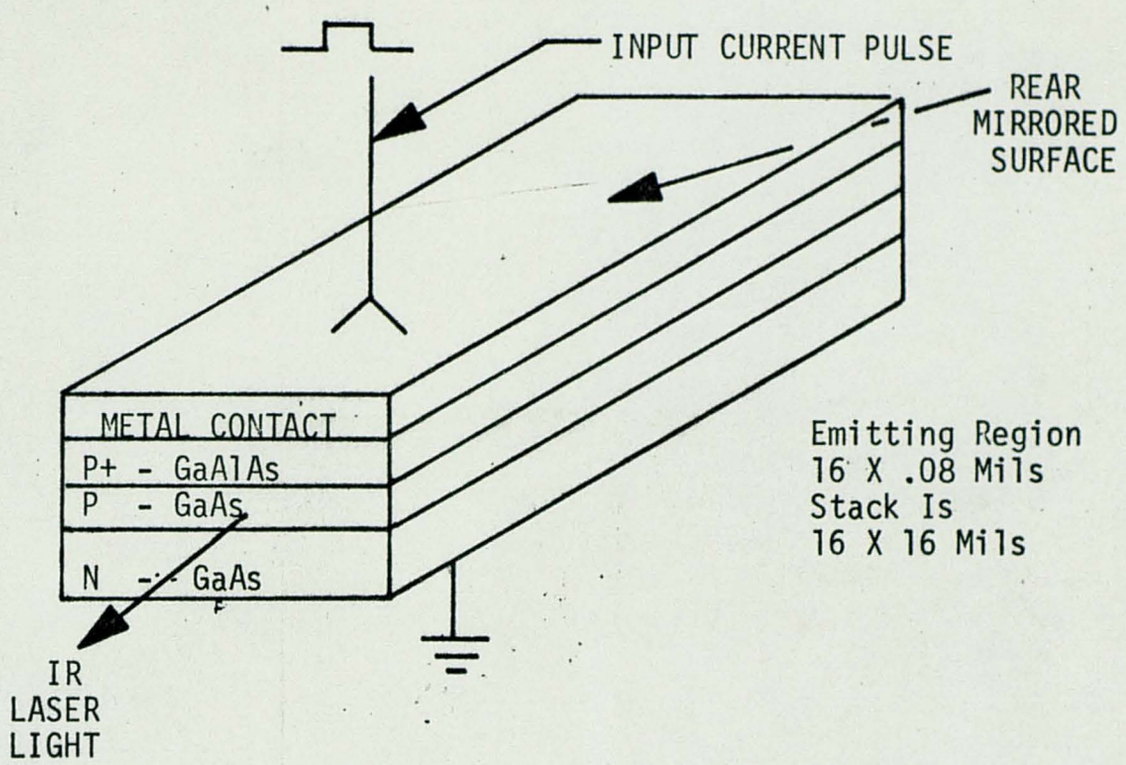

FIGURE 11. Structure of GaAs Semiconductor Laser

This laser emits coherent radiation in the near IR region at 904 nm (27°C) with a spectral bandwidth of 1 nm. The wavelength increases 0.23 nm/°C with increasing temperature.

The laser diode used has a 100 watt peak power pulse in a 180 n.sec pulse width. To achieve 100 watts, six laser diodes are stacked in a series connected array to form a 20 X 20 mil source. The laser is driven with a 100 amp. pulse. The current pulse is generated by an SCR pulser circuit shown in Figure 12.

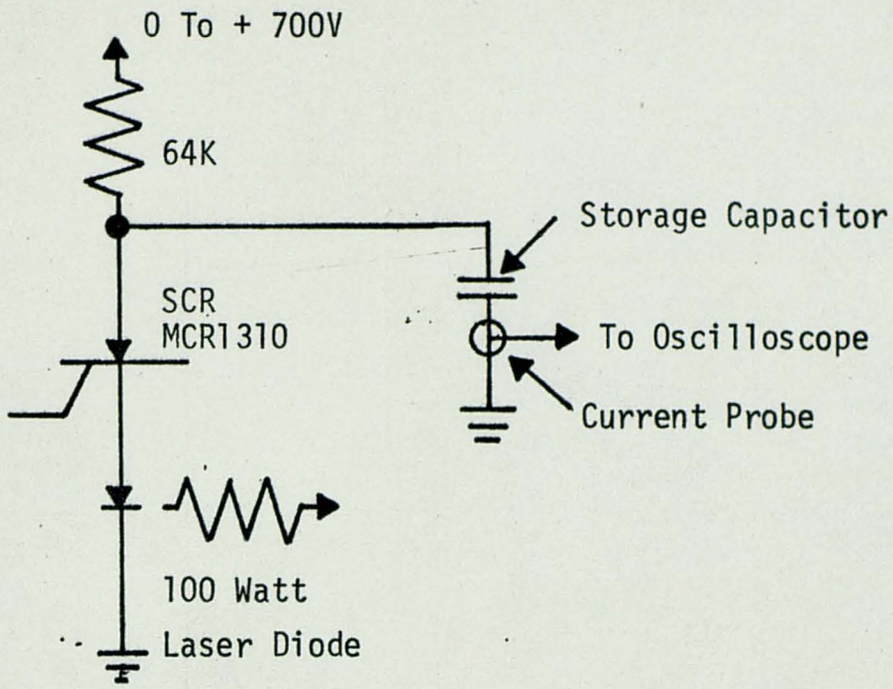

FIGURE 12. Laser Pulser Circuit

The current pulse is generated by discharging the storage capacitor C through the SCR and the laser stack. Rise time of the current pulse is determined by the speed of the SCR, while the fall time is determined by the capacitor value and the total resistance in the discharge circuit. The peak current in the discharge circuit can be controlled by varying the supply voltage; providing the prf is low enough to allow the capacitor to recharge fully between current pulses. Maximum prf is determined by the values of the anode resistor and charging capacitor. When a positive pulse is applied to the gate of the SCR the anode to cathode circuit

impedance drops from an open circuit to a fraction of an ohm. The value of the anode resistor is chosen so that the current through this resistor is below the holding current of the SCR and the circuit acts as a one shot. Once the capacitor C is discharged through the laser the SCR turns off.

The current pulse to the laser diode is monitored using a Tektronix CT-2 current transformer and observing the pulse on an oscilloscope. The laser current pulse is shown in Figure 13.

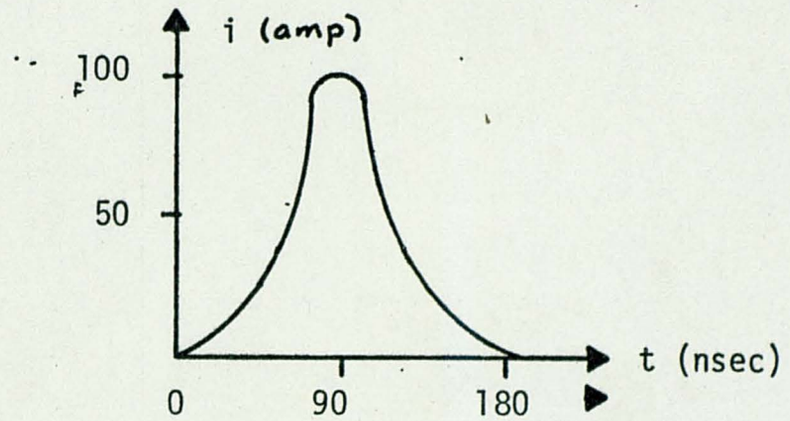

FIGURE 13. Laser Current Pulse

The laser diode radiation pattern in the plane perpendicular to the plane at the junction is 20° at the half radiant intensity points and approximately 10° in the plane at the junction. The transmitter beam is collimated using a Dallmeyer taking lens with a 76mm focal length, f#1.9. To obtain the maximum energy collection, it is necessary to use a low f number lens. To obtain the minimum beam divergence, a long focal length lens is required.

This selection of lens represents a compromise between maximum power and minimum beam divergence.

5. EXPERIMENTAL RESULTS.

The receiver-transmitter system is shown in Figure 14.

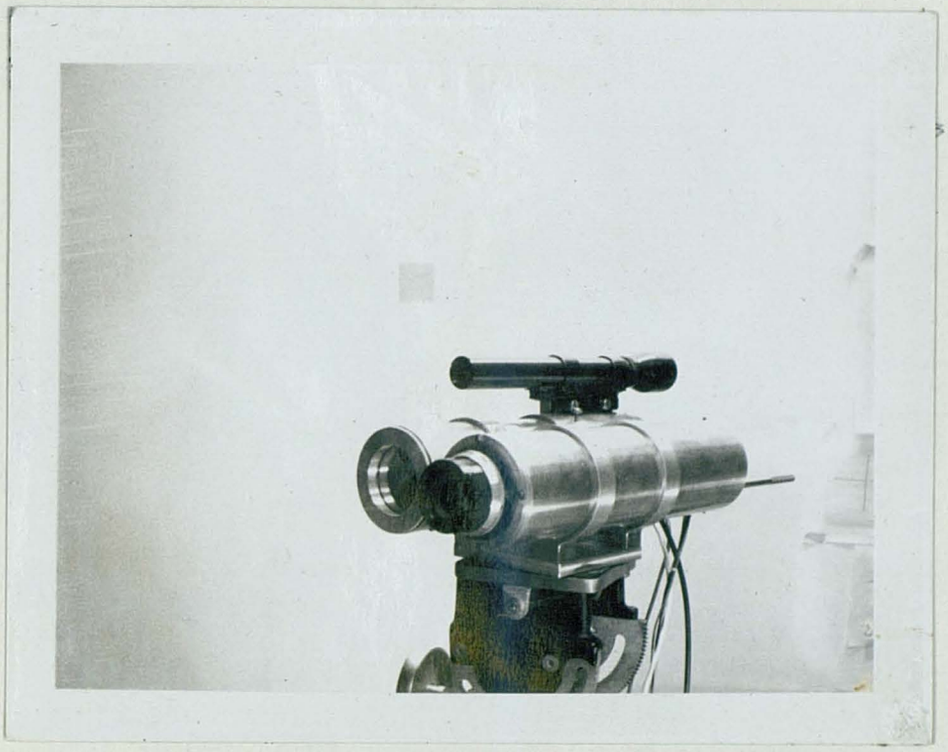

FIGURE 14. Laser Transmitter-Receiver System

In this system it is necessary to align the receiver and transmitter axes prior to recording data. The system was aligned by continuously pulsing the laser at a prf of 300 Hz, and viewing the transmitted laser beam at night with an infrared viewer. The focal length of the transmitter is adjusted until the laser beam

is collimated. The beam diameter at 300 meters is approximately two feet in diameter. A telescope was used as a sighting and aiming device and the laser beam was aligned to the axis of the telescope by aiming the telescope at a light emitting diode (LED) at a range of 300 meters. The laser transmitter collimation lens was then moved mechanically so the beam was positioned on the LED. The receiver axis was next aligned to the system axis by maximizing the received signal as monitored on an oscilloscope. Alignment was accomplished by mechanically moving the receiver lens until maximum signal was obtained.

Table 1 lists various target objects used to evaluate this system; the range to the object, and the signal to noise (S/N) ratio. A calibrated Tektronix 454/A Oscilloscope was used for the S/N measurements. The first four targets are self explanatory. The Scotchlite, 3M, material is a wide angle exposed lens reflective fabric consisting of minute glass spheres bonded to the surface of cotton drill cloth. The fabric is silver-grey by day and appears brilliant silver-white under visual reflected light at night. It is designed to provide reflective brilliance for night time pedestrian safety. Its stated reflective brilliance is 100 times that of flat white paint.

The Scotchlite, 3M, adhesive, retroflective material is designed for use on reflective safety sign.

TABLE 1 - SYSTEM RESULTS

Target	Range (meters)	S/N
a. Pine Tree	212	7
b. Building (Painted Green)	312	12
c. White Shirt	312	14
d. Building (White Asbestos Shingle)	327	17
e. Scotch Lite (Fabric)	312	390
f. Scotch Lite (Adhesive)	312	Receiver Saturation

Using this avalanche detector system, one can detect reflected pulses on a bright sunny day, from targets at a range in excess of 300 meters. Because of the narrow laser pulse width utilized, the laser system is eye safe, on a single-shot basis, and could be utilized for a variety of ranging purposes.

LIST OF REFERENCES

1. Johnson, Kenneth M. "High-Speed Photodiode Signal Enhancement at Avalanche Breakdown Voltage." IEEE Transactions on Electron Devices, Vol. 10, Dec. 1970, p. 324.

2. Todd, C. Zener and Avalanche Diodes. New York: Wiley, 1970.

3. Yariv, A. Introduction to Optical Electronics. New York: Holt, Rinehart and Winston, 1971.

4. Schiel, E. J. "High Gain Silicon Avalanche Detectors." Proceedings of the 1971 Electro-Optical Systems Design Conference. New York, April, 1971.

5. Optoelectronics Data Book for Design Engineers. Houston: Texas Instruments, Inc., 1972.

6. McIntyre, R. "Multiplication Noise In Uniform Avalanche Diodes." IEEE Transactions of Electron Devices, Vol. ED-13, 1965, p. 834.

7. Electro-Optics Handbook. RCA, Technical Series, EOH-10. Harrison, N.J.: RCA, 1972.

8. Kordes, R. "Optimize Photodiode Detector Design." Electronic Design, November 9, 1972, p. 107.

9. Baird, J. "A Model of the Avalanche Photodiode." IEEE Transactions on Electron Devices, ED-14, May (1967), p. 214.